Journal of Volcanology and Geothermal Research 310 (2016) 107–117

Contents lists available at ScienceDirect

Journal of Volcanology and Geothermal Research

journal homepage: www.elsevier.com/locate/jvolgeores

Characterization of the hydrothermal system of the Tinguiririca Volcanic Complex, Central Chile, using structural geology and passive seismic tomography

C. Pavez [a,b,*], F. Tapia [a], D. Comte [b,c], F. Gutiérrez [a,b], E. Lira [e], R. Charrier [a,b,d], O. Benavente [a]

[a] Departamento de Geología, Facultad de Ciencias Físicas y Matemáticas, Universidad de Chile. Plaza Ercilla 803, 13518 Santiago, Chile
[b] Advanced Mining Technology Center, Facultad de Ciencias Físicas y Matemáticas, Universidad de Chile. Avenida Tupper 2007, 8370451 Santiago, Chile
[c] Departamento de Geofísica, Facultad de Ciencias Físicas y Matemáticas, Universidad de Chile. Avenida Blanco Encalada 2002, 8370449 Santiago, Chile
[d] Facultad de Ingeniería, Universidad Andres Bello, Campus República, Santiago. Avenida República 237, 8370146 Santiago, Chile
[e] Departamento de Ingeniería Estructural y Geotécnica, Pontifica Universidad Católica de Chile, Av. Vicuña Mackenna 4860, Macul, 7820436 Santiago, Chile

ARTICLE INFO

Article history:
Received 16 June 2015
Accepted 19 November 2015
Available online 2 December 2015

Keywords:
Tinguiririca Volcanic Complex
Passive seismic tomography
Structural geology
Conceptual model

ABSTRACT

A structural characterization of the hydrothermal–volcanic field associated with the Tinguiririca Volcanic Complex had been performed by combining passive seismic tomography and structural geology. This complex corresponds to a 20 km long succession of N25°E oriented of eruptive centers, currently showing several thermal manifestations distributed throughout the area. The structural behavior of this zone is controlled by the El Fierro–El Diablo fault system, corresponding to a high angle reverse faults of Oligocene–Miocene age. In this area, a temporary seismic network with 16 short-period stations was setup from January to April of 2010, in the context of the MSc thesis of Lira (2010), covering an area of 200 km^2 that corresponds with the hydrothermal field of Tinguiririca Volcanic Complex (TVC), Central Chile, Southern Central Andes. Using P- and S- wave arrival times, a 3D seismic velocity tomography was performed. The preliminary locations of 2270 earthquakes have first been determined using an a priori 1D velocity model. Afterwards, a joint inversion of both, the 3D velocity model and final locations have been obtained. High Vp/Vs ratios are interpreted as zones with high hot fluid content and high fracturing. Meanwhile, low Vp/Vs anomalies could represent the magmatic reservoir and the conduit network associated to the fluid mobility. Based on structural information and thermal manifestations, these anomalies have been interpreted. In order to visualize the relation between local geology and the velocity model, the volume associated with the magma reservoir and the fluid circulation network has been delimited using an iso-value contour of Vp/Vs equal to 1.70. The most prominent observed feature in the obtained model is a large "V" shaped low-velocity anomaly extending along the entire study region and having the same vergency and orientation as the existing high-angle inverse faults, which corroborates that El Fierro–El Diablo fault system represents the local control for fluid mobility. This geometry coincides with surface hydrothermal manifestations and with available geochemical information of the area, which allowed us to generate a conceptual model of fluid circulation in the volcanic–hydrothermal system as well as define the location of the magmatic reservoir.

1. Introduction

Determination of the internal structure of hydrothermal systems is commonly assessed by a combination of geological and geophysical methods including structural analysis and seismic tomography (Muksin et al., 2013; Nukman and Moeck, 2013; Muksin et al., 2014; Spica et al., 2015). Together, they can provide significant information to improve our knowledge regarding the superficial and sub-surface features of active hydrothermal systems by linking regional and local structures, seismicity and mobility of hydrothermal fluids (Foulger, 1982). Considering the amount of regional seismic activity produced in active margins, the volcanic–hydrothermal systems developed in such settings are the most suitable systems to be studied following the aforementioned approach (e.g. Husen et al., 2004; Jousset et al., 2011; Muksin et al., 2013). The existence of deep and intermediate depth seismicity in convergent margins improves the accuracy of the obtained velocity models providing significant evidences of sub-surface features and enabling the illumination of lower areas (Zhao, 2001; Koulakov, 2013). Furthermore, different petro-physical parameters of the host rock such as temperature, composition and density, can be linked to the 3D velocity structure of P and S seismic waves, Vp/Vs ratios and the percentage variations of %dVp and %dVs (Lees, 2007). These variables could also indicate the presence of magmatic reservoirs, and

* Corresponding author at: Advanced Mining Technology Center, Facultad de Ciencias Físicas y Matemáticas, Universidad de Chile. Avenida Tupper 2007, 8370451 Santiago, Chile. Tel.: +56 2 29771008.
E-mail address: cv.pavez.o@gmail.com (C. Pavez).

http://dx.doi.org/10.1016/j.jvolgeores.2015.11.018
0377-0273/

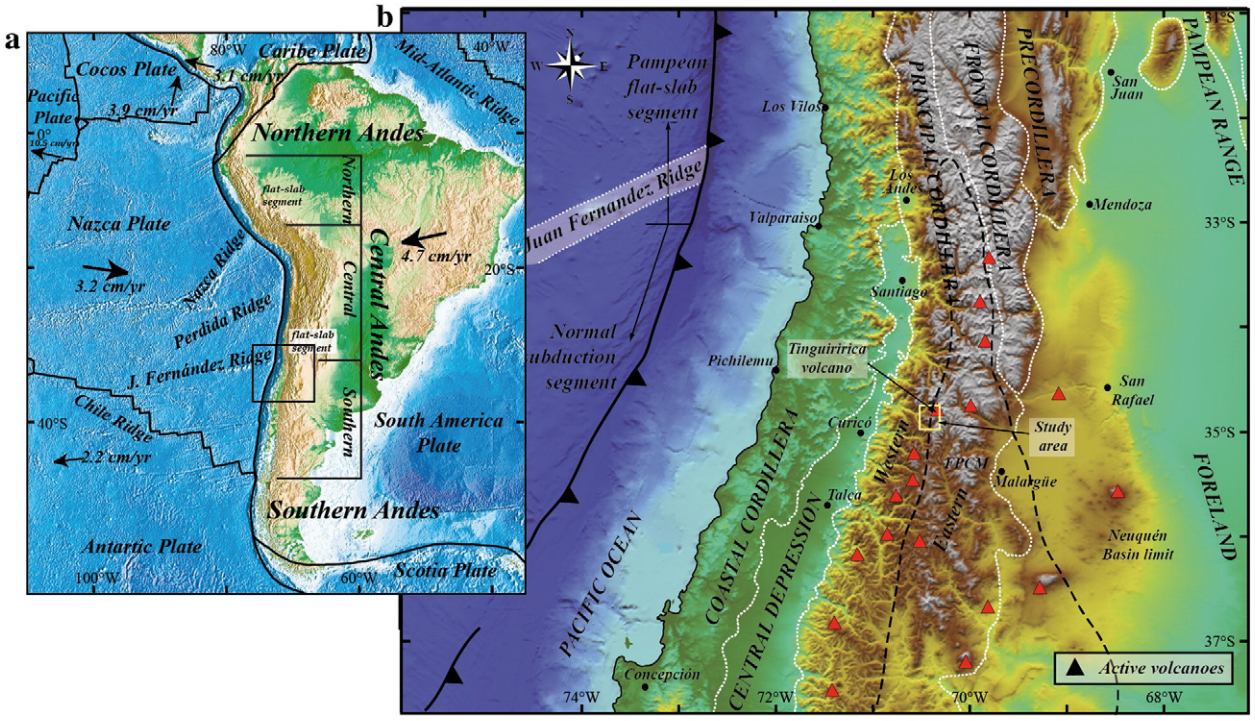

Fig. 1. (a) Digital elevation model map corresponding to an overview of South America. Box indicates the location of the study area. (b) Digital elevation model showing the regional geological context of Central Volcanic Zone. Major physiographic divisions are highlighted. The study area and the Tinguiririca volcano are shown in a yellow square.

distinction between fluid and melt zones in active volcanoes, which could be used as a geothermal exploration tool in volcanic–hydrothermal systems (Koulakov, 2013). A change of the seismic velocities through the medium could also indicate lithological differences (i.e. magmatic intrusions, volcanic deposits, sedimentary sequences), or even the presence of fluids at different temperatures (Lees, 2007). Generally speaking, in volcanic systems, high Vp/Vs (1.75–1.80) velocity anomalies observed in shallow crustal regions represent structural features associated with cooled magma bodies (Lees, 2007). Whereas, low Vp/Vs (1.65–1.70) velocity anomalies are interpreted as evidence of melt accumulation, like magma reservoirs and active conduits of liquids and magma (Lees, 2007). In hydrothermal systems, on the other hand, high Vp/Vs velocity anomalies are usually associated to steam condensation zones, areas where meteoric water infiltrate and zones where hydrothermal gases migrate from the reservoir to distal areas due to increase of effective pressure (Simiyu, 1999; Foulger et al, 2003; De Matteis et al, 2008). In contrast, low Vp/Vs velocity anomalies are related with high temperatures zones, steam saturated formations and zones hydrothermally altered (Foulger and Miller, 1995; Simiyu, 1999; Foulger et al, 2003; Yoshikawa and Sudo, 2004; De Matteis et al, 2008).

The Southern Andes volcanic zone (SVZ) provides one of the best environments for the development of seismic images in active volcanic–hydrothermal systems, because of the occurrence of numerous geothermal areas associated with both seismic activity and active volcanism (e.g. Hauser, 1997; Stern et al., 2007; Farías et al., 2010). Particularly, Tinguiririca Volcanic Complex[1] (hereafter TVC) (Fig. 1), one of these several potential geothermal systems in Central Chile (Benavente, 2015; Benavente et al., 2015), haks especially caught our attention to the great variety of surface thermal manifestations. In fact, this research is complementary to the studies conducted by Lira (2010) in the zone. In the present work, we characterize the TVC and its hosted hydrothermal system. In the first step we use the travel times of P and S waves of local and regional earthquakes to perform a passive seismic tomography of the area. The information derived from the final velocity model (i.e. %dVp, %dVs variations and Vp/Vs ratio) is then coupled with a structural geologic cross section and regional mapping in order to corroborate the link between the local fault system and the velocity anomalies Finally, we create a 3D model of the Tinguiririca volcanic–hydrothermal system using an iso-value contour that covers the whole study area. This 3D model successfully explains the current distribution of the physical and chemical characteristics of the hydrothermal manifestations reported in the area (Clavero et al., 2011; Benavente, 2015; Benavente et al., 2015). This work correspond to the first hydrothermal system analyzed using complementary methods in the Chilean Andes.

2. Geology of the TVC region

The TVC is an active volcanic cluster comprising two major stratovolcanoes, Tinguiririca and Fray Carlos, and several scoria cones distributed along 20 km in N25° E direction. (Fig. 2). Volcanic activity seems to have migrated along the N25° E alignment of volcanic cones, being the eruption registered in 1917 at Tinguiririca volcano the last eruptive episode experienced by the TVC (Arcos, 1987; Gonzalez-Ferrán, 1995; Stern et al., 2007). The volcanic cluster overlies a lower to middle Pleistocene plateau of andesitic to basaltic–andesitic lavas that cover an area of 160 km^2 (Arcos, 1987).

Late Jurassic to Neogene sedimentary and volcanic rocks constituted the basement of the TVC (Fig. 2). The oldest sequence corresponds to the Late Jurassic continental Río Damas Formation (Fig. 2) consisting of ~3800 m thick red conglomerates and sandstones interfingered with andesitic volcanic breccias and lavas (Charrier et al., 1996; Rossel et al., 2014). The marine Baños del Flaco Formation overlies the Río Damas Formation (Fig. 2). It consists of ~370 m thick calcarenites and calcilutites with sandstone intercalations representing a transgressive–regressive cycle during the Late Jurassic–Early Cretaceous (Charrier et al., 1996). Unconformably overlaying the Baños del Flaco deposits is the BRCU (Brownish-red Clastic Unit) (Charrier et al., 1996) (Fig. 2). This is an Early Late Cretaceous continental unit

[1] TVC.

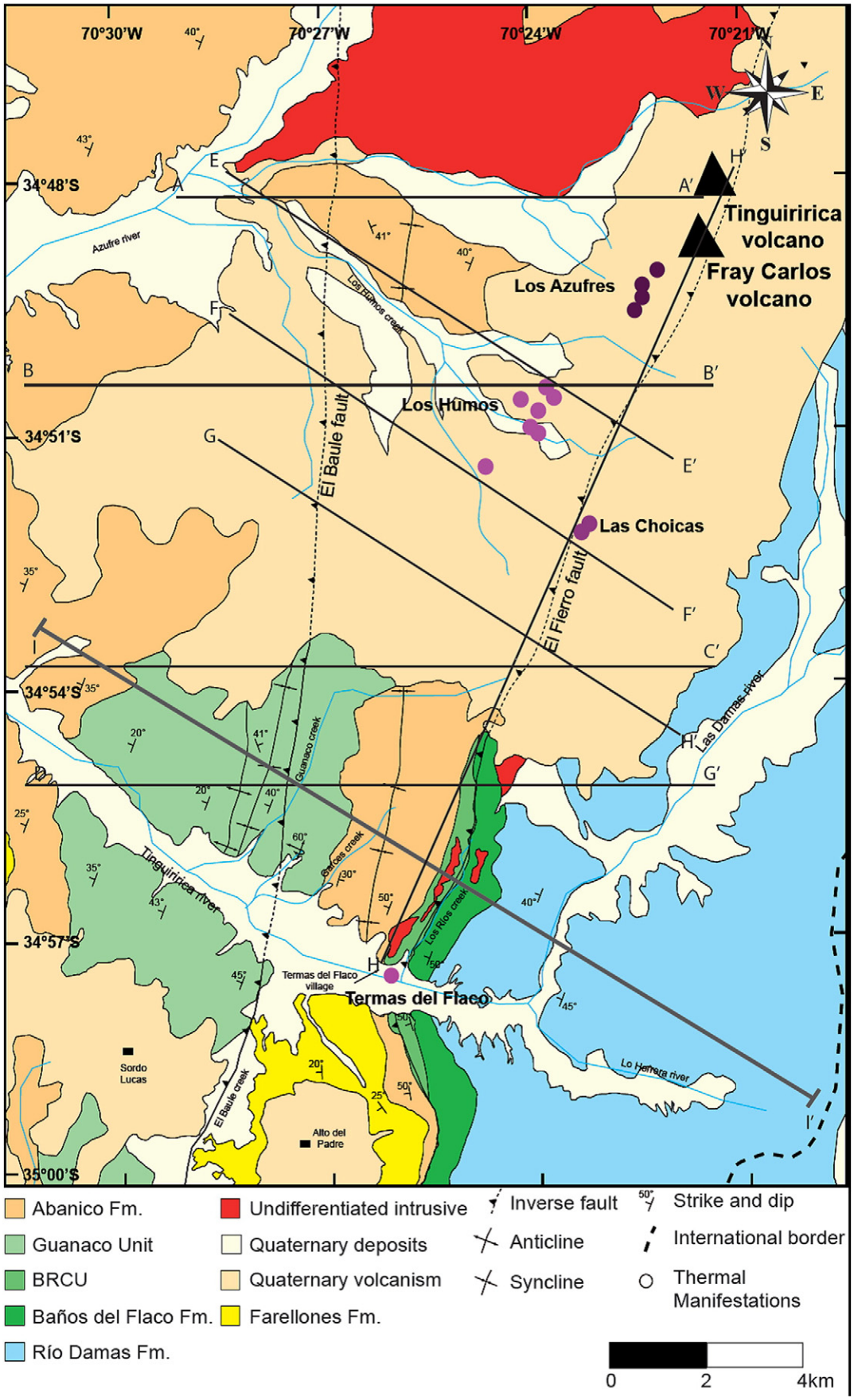

Fig. 2. Geology of the TVC region. Location is in Fig. 1. Solid black lines indicate the location of the cross-sections in Supplementary Material (Fig. S3). Black triangles represent volcanoes. Circles represent hot spring and fumarolic fields identified in this work (Arcos, 1987).

Table 1
UTM coordinates (WGS84-19S), altitude (m.a.s.l.) and description of Termas del Flaco, Las Choicas, Los Humos and Los Azufres thermal manifestations. Coordinates of Las Choicas fumarolic field were taken from Clavero et al., (2011).

	UTM–E	UTM–N	Altitude	Description	Temperature
Termas del Flaco	0368138	6138365	2829	Hot spring	63.7 °C–89.4 °C
Manifestation 1	0371705	6142751	2874	Gas emission	89.2 °C
Manifestation 2	0372656	6142313	3462	Gas emission	88.1 °C
Los Humos 1	0371838	6143067	2975	Fumarolic field	90.6 °C
Los Humos 2	0371612	6143019	2972	Fumarolic field	27.9 °C
Los Humos 3	0371802	6143235	2977	Fumarolic field	90.7 °C
Los Humos 4	0371541	6142686	2873	Fumarolic field	91.3 °C
Los Humos 5	0371250	6142895	2726	Hot spring	59.7 °C
Los Azufres 1	0365995	6148465	1569	Sulfur emissions	–
Los Azufres 2	0368727	6148686	1797	Sulfur emissions	–
Los Azufres 3	0373120	6146230	3157	Hot spring	25.5 °C
Las Choicas 1	0373434	6140198	–	Fumarolic field	Boiling temperature
Las Choicas 2	0373385	6140136	–	Fumarolic field	Boiling temperature

Fig. 3. Thermal manifestations of Tinguiririca Volcanic Complex: (A) Tinguiririca stratovolcano; (B) Termas del Flaco hot springs (T = 63.7 °C − 89.4 °C); (C) Los Humos acid crater lake (pH = 1,87; T = 90.6 °C); (D) Los Humos fumarolic field (T = 90.7 °C); (E) Los Humos bubbling mud pool (T = 89.2 °C); (F) Los Humos hot spring (T = 59.7 °C); and (G) Los Azufres hot springs (T = 27.5 °C).03734346140198.

consisting of a basal breccia, conglomerates and conglomeratic sandstones alternating with mudstone and fine sandstone intercalations. In the southern slope of the Tinguiririca river valley, the unconformity separating the BRCU from the overlying Paleogene Abanico Formation is well exposed (Fig. 2) (Charrier et al., 1996).

To west of the Termas del Flaco village, along the slopes of the Tinguiririca river valley, two mostly volcanic units are exposed that have been grouped in the Late Cretaceous Guanaco volcanic unit and in the Eocene–Oligocene Abanico Formation (Fig. 2). The former unit corresponds to a 1200 m thick succession of bimodal volcanism consisting of dacitic to rhyolitic tuffs, basalts, basaltic andesites and andesites with intercalations of volcanoclastic breccias and sandstones (Mosolf, 2013). The latter consist of 1000 m of volcanoclastic deposits and acidic to intermediate lavas with intercalations of coarse and fine-grained detrital deposits and lacustrine limestones (Charrier et al., 1996, 2002). The Abanico Formation unconformably overlies the Late Cretaceous Guanaco volcanic succession. The Abanico Formation is covered by a thick ignimbritic deposit followed by thick, coarse conglomeratic layers and sandstones assigned to the Farellones Formation (Tapia, 2015). Pleistocene–Holocene arc-related rocks unconformably cover all the previous stratigraphic units and have been grouped in the Tinguiririca Volcanic Group (Arcos, 1987; Charrier et al., 1996) (Fig. 2).

Thermal activity at TVC occurs in a roughly N–S band on the W and SW slopes of Tinguiririca volcano and resembles the typical features of high-temperature and elevation ($T > 200$ °C) volcanic-hosted hydrothermal systems, i.e. high-elevation fumaroles and low-land chloride-rich springs (Goff and Janik, 2000). Four hydrothermal areas have been reported at TVC: (1) Los Azufres, (2) Los Humos, (3) Las Choicas and (4) Termas del Flaco (Clavero et al., 2011; Benavente, 2015; Benavente et al., 2015). The first three areas, located between 2700 and 3300 m a.s.l., are characterized by sporadic fumarolic discharges, mud pools, sulfate-rich steam-heated waters (Clavero et al., 2011; Benavente, 2015; Benavente et al., 2015). All the fumarole discharge mainly steam (>90% mol/mol) at boiling temperatures (~90 °C) and are associated with acid-sulfate alteration and native sulfur deposits (Benavente, 2015). The main outflow of these geothermal systems can be found at Termas del Flaco, ~16 km to the south of TVC, where high-temperature (between 63.7 and 89.2 °C), Cl-rich waters are discharged at an elevation of 1720 m.a.s.l., ~1600 m lower than the Las Choicas fumarolic field (Table 1). The water has a neutral pH, a Na–Cl composition with TDS of up to 4000 mg/L and a stable isotope composition ($\delta^{18}O$– and δD–H_2O) that resemble local meteoric water, and is associated to a gas phase showing relatively high concentrations of CH_4 (Benavente, 2015; Benavente et al., 2015).

According to Benavente (2015), fumarolic discharges at Los Humos area are characterized by the absence of magmatic gaseous compounds (SO_2, HCl, HF) and $\log(H_2/H_2O)$ values close to −2.82, which indicate that these fumarolic fluids get equilibrated at depth in a vapor phase under typical (non-magmatic) hydrothermal conditions (Giggenbach, 1987). Nevertheless, the occurrence of significant mantle He in the fumarolic and bubbling pool gases at Los Humos and Termas del Flaco, respectively (R/R_{air} values ranging from 2.13 to 3.9), as well as the presence of non-atmospheric N_2 in both zones (N_2/Ar ratios up to 233) suggests the occurrence of an active deep magmatic system underlying the upper hydrothermal zone (Benavente, 2015; Benavente et al., 2015). The presence of H_2 and H_2S in the fumarolic discharges evidences reservoir temperatures in excess of 250 °C, which is consistent with the temperatures estimated by using the CO_2–Ar and CO_2–CH_4 geothermometers (~270 °C; Benavente, 2015; Benavente et al., 2015). The high Cl and Li concentrations (~1800 and ~4 mgL^{-1}), as well as the Cl/B ratio (~80) of the Termas del Flaco water also suggest that these fluids are derived from a high temperature reservoir (Benavente, 2015; Benavente et al., 2015). Geothermometric calculations in the Na–K–Ca–Mg system indicates that these Cl-rich waters get equilibrated at a temperature close to 230 °C (Benavente, 2015; Benavente et al., 2015), which is consistent with the maximum temperature measured at the bottom of the ~800 m depth slim hole drilled close to Los Humos area (Clavero et al., 2011). The Cl-rich springs cannot be conclusively linked to a source beneath Los Humos and Las Choicas areas, but if they were connected, the ~40 °C difference between the temperatures estimated for the Cl-rich and fumarolic discharges may suggests that these Cl-rich water have moved laterally a considerabledistance discharging at surface.

2.1. Structural geology data of the basement of the TVC

From a regional point of view, this Andean region corresponds to the internal part of the fold-and-thrust belt that characterizes the eastern slope of the Andean orogen (Kley et al., 1999; Ramos et al., 2004).

In order to determine the structure of the area, we describe next the main structural features of the study region, complemented with information from previous studies (Charrier et al., 1996, 2002; Mescua et al., 2014). This allowed the construction of a schematic cross section (Fig. 4) constrained only by surface data because the geothermal borehole information gathered in the area is not available.

In the eastern sector of the TVC (Fig. 2), the west dipping Mesozoic successions (Fig. 5A) make up the back-limb of a large, east-vergent anticline of 10 km half-wavelength with a front-limb located east of the

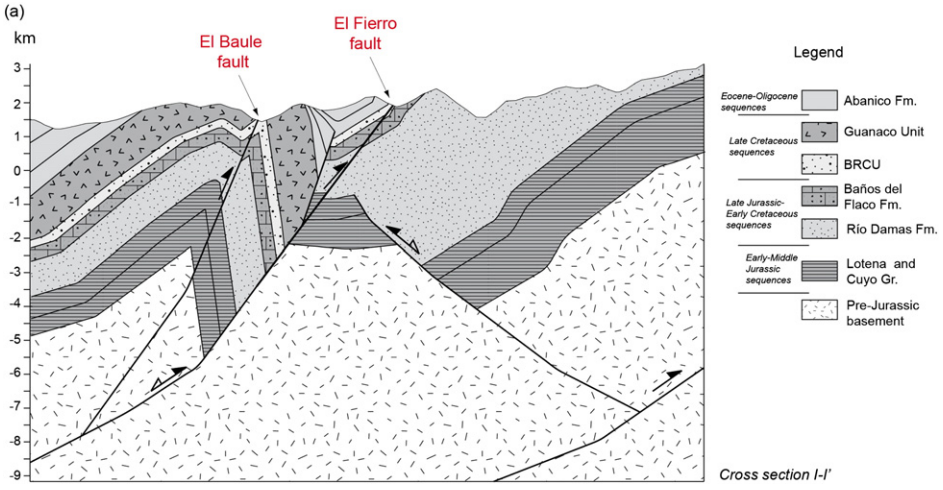

Fig. 4. Schematic cross section I-I′. See Fig. 2 for location. The cross section shows the deep interpretation of the out-cropping structures along the TVC region (see text for further explication).

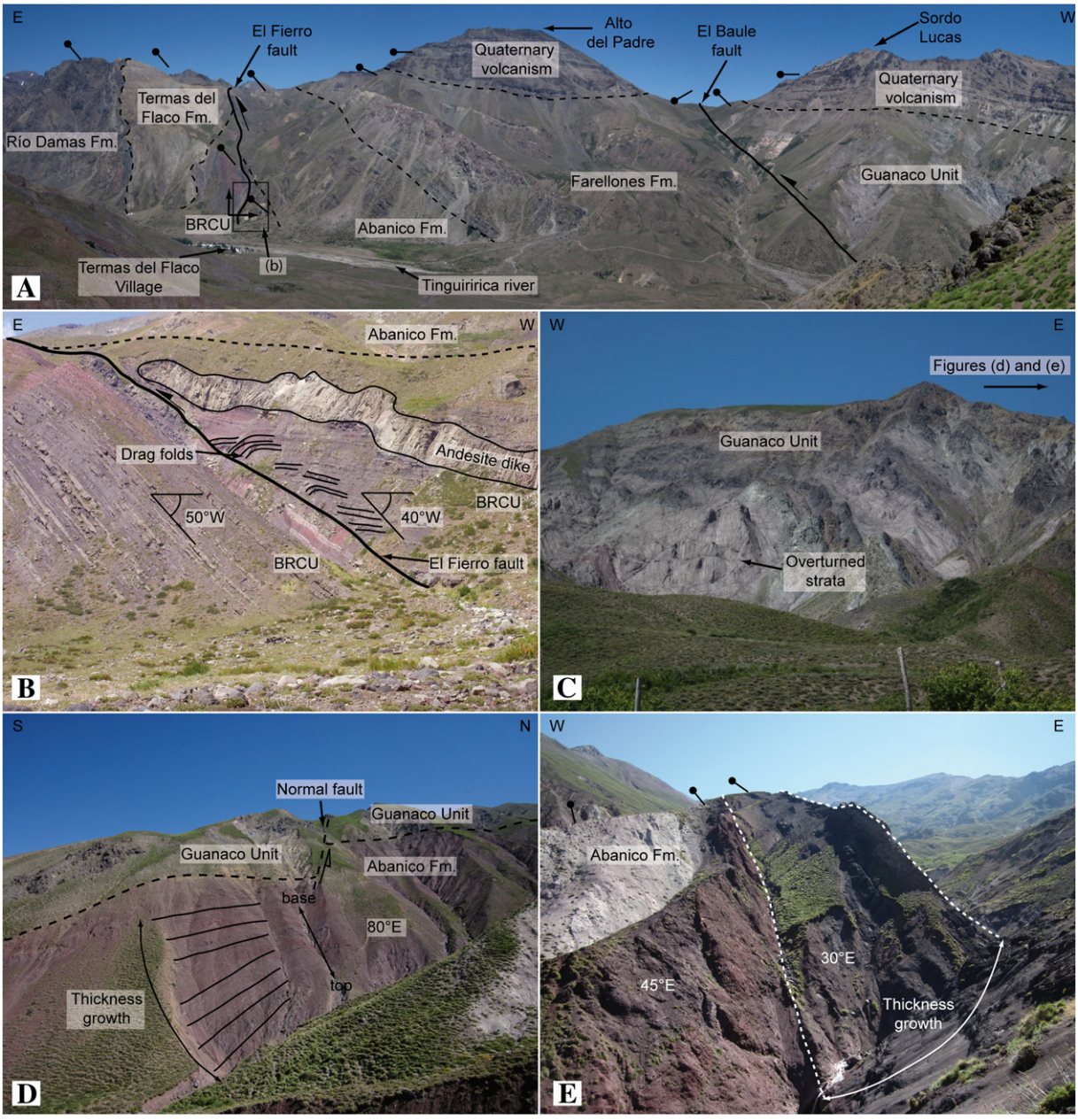

Fig. 5. Main structural features of the TVC region. (A) Southward view of the structure in the southern slope of the Tinguiririca valley. (B) Drag folds in the BRCU unit associated with El Fierro fault deformation. See Fig. 4 for location. (C) Frontal flank of the anticline along the northern slope of the Tinguiririca valley. Note the overturned strata of the Late Cretaceous volcanic sequences. (D) Unconformity between Late Cretaceous and Abanico Formation rocks. The Paleogene rocks show growth strata associated with the synorogenic deposition. Note also the normal faults that accommodate the thickness of the Abanico Formation. (E) Growth strata of the Abanico Formation developed in the frontal limb of the northern anticline.

study area (Mescua et al., 2014). According to these authors, in the core of the anticline crop out complexily thrusted and folded Early Jurassic marine deposits. Moreover, these authors interpreted this fold as a structure associated to the inversion of normal faults associated with the development of the extensional Mesozoic Río del Cobre depocenter. The inverted normal fault dips to west rooting in a detachment at 10 km depth and, thus, tilting westward the Mesozoic rocks and structures of the western sector of the study area (Mescua et al., 2014) (Fig. 4).

The western sector is characterized by the presence of the ~9 km half-wavelength anticline well exposed along the northern slope of the Tinguiririca river valley (Fig. 2) involving the Late Cretaceous volcanic sequences and the Abanico Formation rocks in the core and limbs respectively. This structure shows a geometry characterized by a short front-limb with overturned strata and a long back-limb (Fig. 5B) indicating an eastward vergency. In the frontlimb the Abanico layers show a progressive unconformity and eastward thickness growth (Fig. 5C & D). On the other hand, a west dipping homoclinal fold involving both the Late Cretaceous volcanic sequence and the Abanico Formation crops out along the southern slope of the valley (Fig. 5A). Considering that the Abanico Formation was deposited during an extensional event (Charrier et al., 1996, 2002, 2005), we infer the presence of a blind west-dipping normal fault system in the Garcés creek area that would be responsible for the progressive unconformity and the eastward growth of the Abanico strata (Fig. 4). Furthermore, the 9 km half-wavelength anticline would be associated with the inversion of the normal fault (cf. Mescua et al., 2014).

The anticline along the northern slope of the Tinguiririca valley is cut by the El Baule faults (Charrier et al., 2002), a N–S east vergent reverse fault mapped along the El Baule creek (Fig. 2). This fault cuts the hinge of the anticline evidencing that it formed after the folding. In the deep,

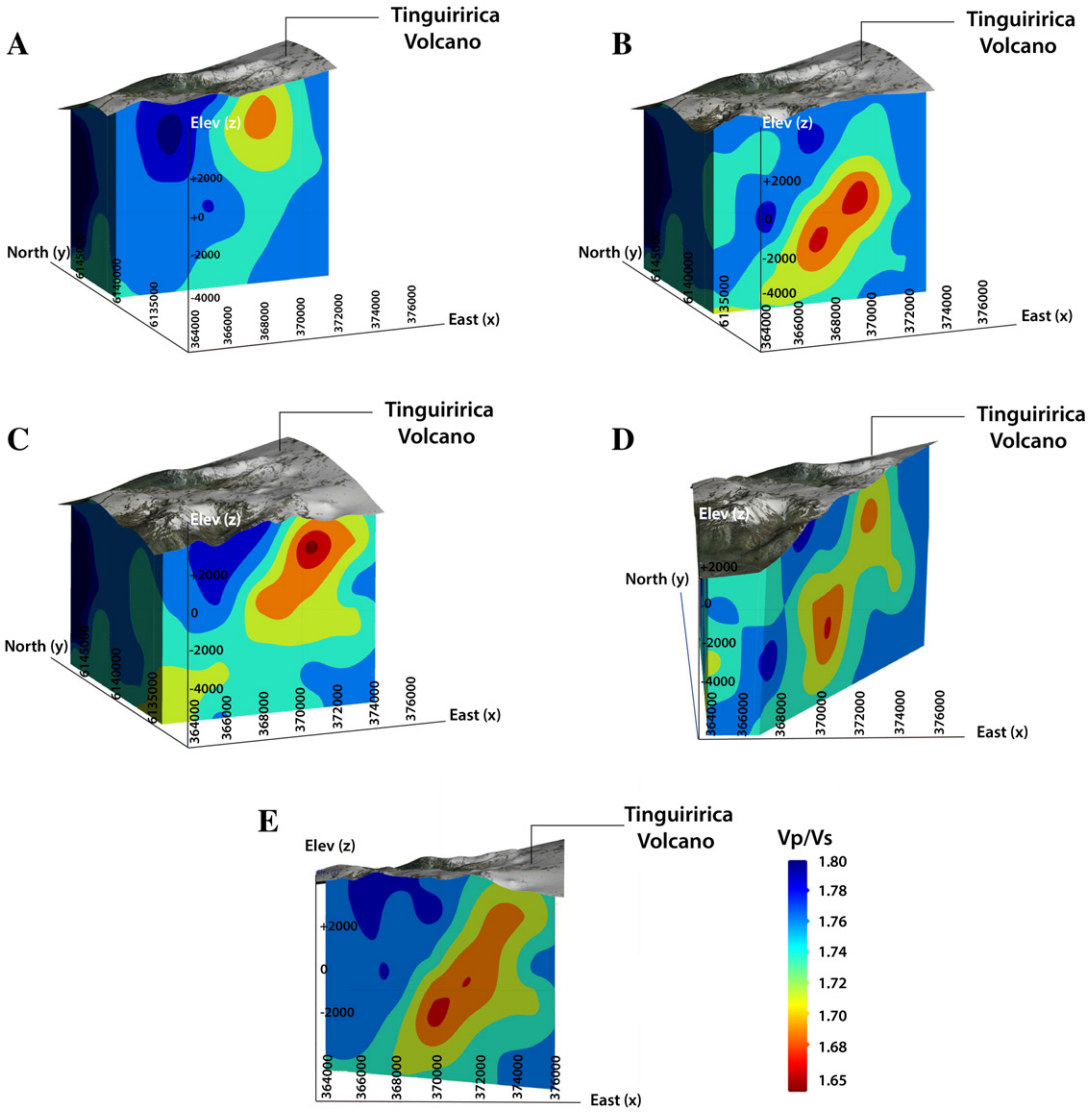

Fig. 6. Local scale cross sections with 3D projection showing velocity structures of the Tinguiririca Volcanic Complex. All sections using the same color palette for velocities. (A), (B), (C) west–east cross sections showing final Vp/Vs velocity model. Each of the sections is separated by 3 km (D) north-east cross sections showing final Vp/Vs velocity model. (E) South-east cross sections showing final Vp/Vs velocity model.

this structure would be connected to the blind inverted extensional fault forming only one fault below 8 km depth (Fig. 4).

The easternmost structure in this region corresponds to the reverse El Fierro fault. It has a NNE–SSW strike, east-dipping slightly oblique to the stratification and thus cutting progressively younger units southward (Fig. 5E). In the southern slope of the Tinguiririca valley, the folds in the BRCU above the El Fierro fault indicate an inverse displacement of the structure (Fig. 5E). According to the characteristics, we interpret the El Fierro fault as a short-cut fault associated to the inverted structure of the Abanico basin (Fig. 4).

3. Local earthquake tomography

In order to achieve a more accurate characterization of the hydrothermal system, a 3D body wave velocity model was determined to define the role of the aforementioned structures in the hydrodynamics of the system and to locate the possible source of heat that would be related to the temperature pattern of the thermal manifestations in the study region (Table 1).

The velocity model was obtained using P- and S-wave arrival times recorded by 16 short period, three components seismic stations deployed on the western flank of the Tinguiririca volcano from January to April 2010 (Lira, 2010). The seismic network covered an area of 20×10 km^2, the average distance between the stations was ~3 km, and 15,000 seismic events were recorded, where ~73% corresponded to the aftershock sequence of the Mw = 8.8 Central-South Chile earthquake (February 27th, 2010), and 27% to local seismicity; in summary 11.343 P- and 11.250 S-wave arrival times, were used in the inversion, respectively.

The seismicity was initially localized using HIPOINVERSE (Klein, 1978), based on a layered 1D velocity model for P waves (Thierer et al., 2005) (See supplementary material, Fig. S1); the 1D-S wave velocity model was obtained using the ratio Vp/Vs = 1.75. The 3D body wave velocity model was obtained in a grid of 390 blocks, covering a volume of $15 \times 18 \times 18$ km^3 in which Vp and Vs are inverted independently. The region was laterally parameterized by 3×3 km^2 grid spacing, and 1–1.5 km depth separation, in 13 layers, ranging from 3 km above sea level to −15 km below.

The hypocenter locations obtained from HYPOINVERSE were used as starting values for the tomography inversion (Roecker, 1982; Roecker et al., 1987; Roecker et al., 1997). After 5 iterations, we obtained ~5% of variation of the model with respect of the previous iteration (See supplementary material, Fig. S2), and 705 blocks were kept from the 780 total initial one.

3.1. Body wave velocity model

Based on the geological information of the study area, Fig. 8 shows 5 cross sections that are crossing the area in 3 different directions: west–east (Fig. 6A, B, C), north–east (Fig. 6D), and south–east (Fig. 6E). The west–east cross sections were built in order to define the hypothetical link between the observed structures and thermal manifestations (Fig. 2) with possible velocity anomalies. The second plane, corresponding to the observed surface orientation of El Fierro fault (Fig. 2), is selected to demonstrate the influence of the main fault plane on the fluid mobility in the system. Finally, the third plane, perpendicular to El Fierro fault, pretends to define the lateral extension of the velocity anomalies around the fault.

In the northern part of the TVC, low Vp/Vs values are identified (Fig. 6A). These values, in the range of 1.65–1.70, predominate to a depth of ~3–4 km below sea level. Meanwhile, southward these anomalies become deeper, reaching 5 km below sea level (Fig. 6B). In the southern part, two different anomalies, separated by a plane-like structure are observed: a dominantly high Vp/Vs values (1.775–1.80) west and a low value anomaly (1.650–1.700) east to the structure (Fig. 6C). In the NE profile, which follows the direction of El Fierro fault (Fig. 6D), is easily recognizable a high velocity anomaly (1.775–1.800) next to a low velocity anomaly (1.650–1.700) from SW to NE. Finally, Fig. 6E shows that the lateral extension of the low velocity anomaly around the fault is ~3 km.

4. Discussion

4.1. Integrated model

In order to integrate the information obtained from the seismic tomography and the structural model, both methods have been made to overlap at the same cross section in the southern zone of the study area (Figs. 2 & Fig. 7). The structural section used for the comparison contains structures that coincide with the major domains identifiable in the velocity model. Minor faults and lithological separations have been omitted because they are not perceptible by the resolution of seismic tomography.

Firstly, the region corresponding to high Vp/Vs ratios (1.750–1.800), coincides with the area enclosed by El Baule and El Fierro faults (Fig. 7B). Due to the proximity of these structures, this zone would correspond to a damage zone which confirms our hypothesis of the existence of high levels of fracturing. In fact, the observed anomaly has the same inferred orientation of both faults at depth. The most significant percentage variations, in this case, are associated with the percentage variation of Vp (Fig. 7C), which in turn is associated with a decrease of the incompressibility elastic modulus (κ). Surrounding this zone, and following the trace of the faults, a low Vp/Vs anomaly (1.650–1.725) is observed (Fig. 7B). This contour may indicate the path of ascent of hot fluids after their possible interaction with a deep magmatic reservoir. From Fig. 7C & d a decrease in %dVs with respect to the area between El Baule and El Fierro faults, which suggest the occurrence of a large amount of hot fluids in motion, is clearly distinguishable.

An intermediate low Vp/Vs ratio is shown (1.725–1.750) in the NE sector of the section. Such values match with a high-permeability zone associated with sedimentary sequences, corresponding to the Río Damas Formation (Fig. 3). This area also exhibits sectors with high Vp/Vs ratios, equally explained by the level of fracturing. Due to the aforementioned features, the Río Damas Formation seems to be acting as the hydrothermal reservoir. Moreover, these rocks are isolated between impermeable marine sequences of both overlying Baños del Flaco and the underlying Lotena Group (Fig. 4). Deeper areas exhibiting relative high velocity values would correspond to the pre-Jurassic basement shown in the structural section (Fig. 7A & B).

The cross-comparison between the structural modeling and the body wave velocity model indicates that the main structures through which hydrothermal fluids are circulating are El Baule and El Fierro faults and their detachment zone at depth (~8 km; Fig. 7). According

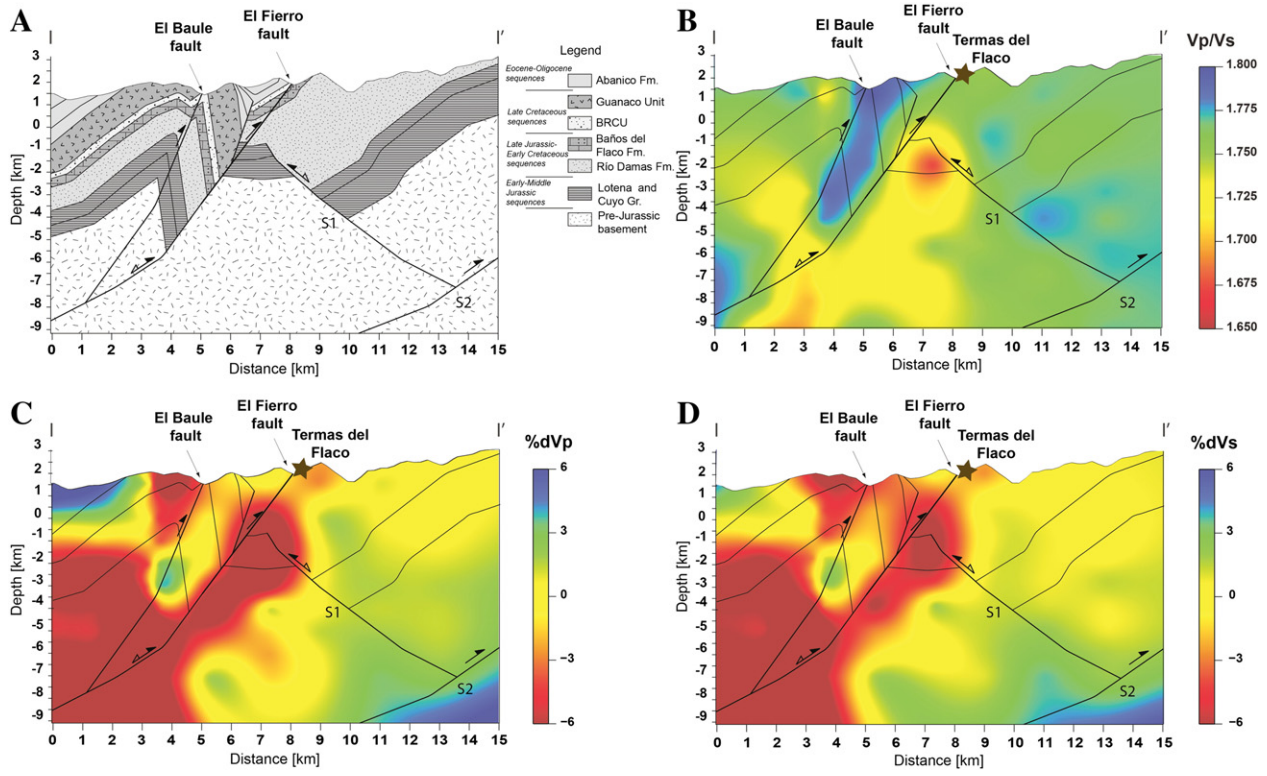

Fig. 7. (A) Schematic cross section I-I′. See Fig. 2 for location. The cross section shows the deep interpretation of the out-cropping structures along the TVC region (see text for further explication).

to these proposed fluid path, these zones have the appropriate features to accommodate a magmatic heat source. The secondary faults S1 and S2 (Fig. 7) shown in the cross section do not seem to play a significant role in the recharge of the reservoir.

4.2. Conceptual model

Based on the exposed seismicity distribution, the Vp/Vs structure of the velocity model and the geologic and tectonic information, a 3D visualization of the magmatic-hydrothermal system was developed. In order to observe the geometry and the latitudinal spatial variations of the low Vp/Vs anomalies, velocity iso-values between the range of 1.65–1.70 were selected. These values define the 3D shape of the anomaly increasing in volume as we approach to the maximum value. Finally, an iso-surface considering a Vp/Vs ratio equal to 1.70 was built. The most prominent feature observed in the obtained model is a large "V" shaped low-velocity anomaly (Fig. 8A & B) which extends along the entire study area. The orientation of this low Vp/Vs anomaly has the same vergency as the El Fierro fault, corroborating the fact that hydrothermal fluids use this fault zone to rise to the surface (Ward and Jacob, 1971; Combs and Hadley, 1977). Using this 3D visualization, it is possible to explain the link between the subsurface and surface results. The location of hot springs and fumarolic fields coincides with the surface expressions at Los Azufres, Los Humos, Las Choicas, and Termas del Flaco (Fig .2). In fact, the borders of the V-shaped low-velocity anomaly are clearly related with fluid discharges located at the surface. Regarding the last point, Fig. 8A shows that sectors 1 and 3 coincide with the location of the Termas del Flaco and Los Azufres thermal features.

In the case of the northern anomalies, the low Vp/Vs ratio (1.65–1.70) coincides with both Los Humos and Los Azufres areas. The behavior of Los Humos fumarolic field is clearly defined by the percentage variation of Vp (See supplementary material, Fig. S3). The last suggest a strong dependence of the incompressibility modulus (κ) since this area is characterized by the occurrence of high temperature degassing activity and hydrothermal alteration. Meanwhile the behavior in the Los Azufres area would be explained by the presence of fluids that could saturate the fracture zone, causing a decrease of both Vp and Vs velocities and triggering the observed hot springs. Although Clavero et al. (2011) have reported high temperature fumaroles in this area, these thermal manifestations were not observed in the present field work. For the southern anomalies, coincident with the Termas del Flaco area, the increase in the Vp/Vs ratio indicates the presence of fluids in a porous and fractured media. Otherwise, in the adjacent anomaly, the low Vp/Vs ratio could be associated with a high temperature fluid content, exhibiting the same behavior as the northern sector (Fig. 6).

(1) With the previous information and the available geochemical data, a conceptual model of fluid circulation at the volcanic–hydrothermal system was generated. Our integrated conceptual model indicates that geothermal activity at TVC displays the typical seismic, geological and geological features of high-temperature and -elevation (T > 200 °C) volcanic-hosted hydrothermal systems (Fig. 8) and is summarized as follows: The heat source of the hydrothermal system corresponds to an intrusive body associated to the volcanic activity recorded for the TVC in the last century. This magma reservoir, having most likely an andesitic composition, would be emplaced between 3 to 6 km b.s.l. as imaged from the low value Vp/Vs anomalies.

(2) Primary fluids originating from magma degassing are scrubbed by an overlying hydrothermal reservoir that would be emplaced within the Rio Damas rocks under the Los Humos and Las Choicas areas. These fluids and the geochemical signature in the zone confirm the existence and the location of the proposed magmatic reservoir, allowing to establish the difference between magma and hot fluids, and supporting the interpretation of the velocity model.

(3) This magma reservoir would lie under a clay cap layer located between 2 and 3 km a.s.l. as was observed by Clavero et al. (2011), who describes the occurrence of a subtle concave-shape conductive layer under the Fray Carlos volcano.

(4) This hydrothermal reservoir would have a liquid-dominated zone at the bottom and an upper zone that is vapor-dominated as a result of a boiling process in deeper parts of the reservoir. Gases (mainly steam and CO_2) from the vapor-dominated zone

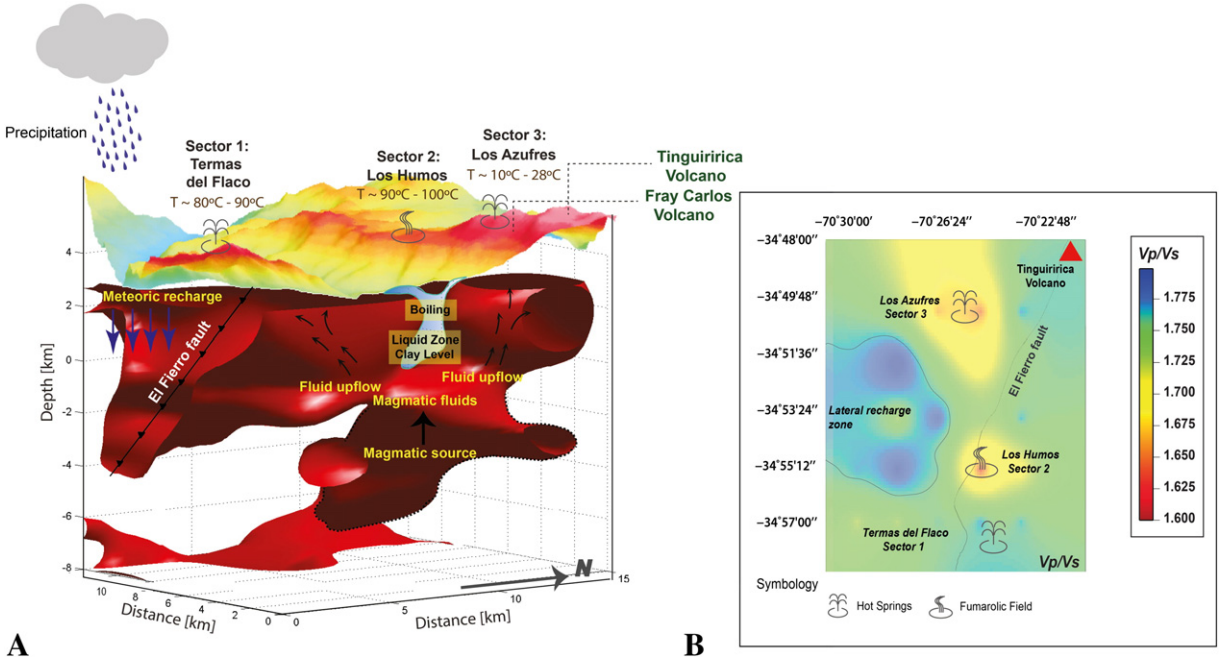

Fig. 8. (A) Perspective view of the 3D model of low Vp/Vs values with topography. In the diagram, the hypothetical fluid mobility in depth and the upflow paths are shown. The iso-ratio surface it was chosen considering Vp/Vs equal to 1.70. (B) In the inset is observed a top view of a horizontal projection of the velocity model at 1.5 km above sea level. In both images sector 1, 2 and 3 correspond to Termas del Flaco, Los Humos and Los Azufres, respectively.

are transferred to the surface and are discharged by the fumaroles, mud pools and minor steaming grounds located at sector 2 and 3 (Los Humos and Las Choicas). Condensed steam, with oxidized H_2S gas, would feed the minor hot acid springs at Los Azufres.

(5) Cl-rich springs from sector 1 (Termas del Flaco) would be originated in the upper part of the liquid-dominated zone located under sector 2 and 3 at an altitude < 1600 m higher than its discharge points at the Tinguiririca valley (~1750 m a.s.l.). These Cl-rich waters would move laterally a considerable distance (~15 km) to the south through a highly fractured zone associated to the El Fierro fault system (Fig. 8).

In general, the obtained results associated with the body wave velocity model are in good agreement with that obtained by Lira, 2010. However, and considering that the low Vp/Vs anomalies were not connected in the Vp/Vs model of Lira (2010), it was impossible for him to explain the dynamic of the system. In our case, we interpret the low Vp/Vs values as a single giant low velocity anomaly that covers the entire study area, allowing us to establish the relationship between this deep anomaly with all the shallow thermal manifestations. Regarding this, both models coincide that the Los Azufres, Los Humos and Las Choicas (not mentioned in Lira (2010)) corresponds to an upflow zone, however, in this work we point out that Termas del Flaco is an outflow area. In the same way, this model allowed the identification of the recharge zone of the hydrothermal system (Fig. 8B). In this context, high Vp/Vs values in the western zone of the study area (Fig. 8B) has been interpreted as a lateral recharge zone, disregarding the possibility that these anomalies are related with hypabyssal intrusions of Cretaceous age (Lira, 2010).

From the point of view of structural geology, the results that emanate from the passive seismic tomography remain consistent with the local geology. Additionally, a low porosity parameter Vp * Vs (Lira, 2010) in areas corresponding to low Vp/Vs values would indicate high porosity, which support the considerable level of fracturing interpreted between El Fierro and El Baule faults. Despite this fact, this interpretation can be enhanced by linking the local structures at depth through the detachment zone, which allowed us to relate the magmatic reservoir with the fault system. Both models (Lira, 2010 and this work) suggest that the reservoir should be located in the Rio Damas Formation, however, we conclude this based on the structural analysis and Lira (2010) based on porosity analysis; the system would be sealed and isolated by the Baños del Flaco and Lotena Group impermeable marine sequences.

Finally, in the context of geochemical analysis, the presence of non-atmospheric N_2 suggests the presence of an active magmatic system that is located beneath the hydrothermal zone. This is also associated with an increase of the Vp/Vs values above the potential magmatic reservoir that help us to assume the existence of a clay level (Fig. 8B; See supplementary material, Fig. S3). This magmatic reservoir, located in the lower lobe of the V-shaped low velocity anomaly (Fig. 8A), could be acting as a heat source of the whole system. On the contrary, Lira (2010) said that the anomaly cannot be associated to the presence of a potential heat source, because in that case it should be expected low Vp and low Vs values, but high Vp/Vs ratios because the temperature of the rock should be close to the partial fusion temperature.

5. Conclusions

(1) This work presents an integrated model based on structural modeling and seismic tomography, which helped to characterize accurately the current background behavior of the Tinguiririca Volcanic Complex. Both methods were correlated using a cross section located in the southern zone of the study area, near Termas del Flaco. This comparison corroborates the primary role of the El Fierro and El Baule faults in the mobility of the hydrothermal fluids in the region, and also allowed the identification of the velocity anomalies related to the presence of hot fluids, in the range of 1.65–1.70.

(2) Using this information it was possible to create a 3D model that indicates the dynamics governing the entire hydrothermal system. The obtained geometry, related with the circulation pattern of fluids, fits well with the location of the surface thermal manifestations. The model suggests that the Termas del Flaco springs correspond to an outflow zone, whereas Las Choicas, Los Humos and Los Azufres are related to upflow zones of hydrothermal fluids (Fig. 8). Both zones seems to be linked to a two-phase hydrothermal reservoir that would be sited within the Rio Dama Formation. Water and gas chemistry suggest reservoir temperatures in the range of 230 and 270 °C. Heat source would be related to andesitic magmatic chamber associated with Fray Carlos, Tinguiririca and/or Montserrat volcanoes likely emplaced between 3 to 6 km b.s.l.

(3) A continuous integration between geological and geophysical methods becomes essential to properly locate possible areas for exploitation projects and for the estimation of the effect of fluid injection in the zone.

Supplementary data to this article can be found online at http://dx.doi.org/10.1016/j.jvolgeores.2015.11.018.

Acknowledgments

The authors would like to thank Energía Andina for providing the unique opportunity to study the Tinguiririca Volcanic Complex. C.P is grateful for the guide and support supplied by Jesús Gomez, René Espinoza & Oscar Castillo. The development of this article was funded by the doctoral fellowship Mecesup, project UCH0708 and by FONDECYT project Nº 1130071. Finally, we thank the support of the Advanced Mining Technology Center (AMTC), Proyecto Basal Nº FB0809.

References

Arcos, J., 1987. Geología del Cuadrángulo Termas del Flaco, Provincia de Colchagua, VI Región, Chile (In Spanish) Memoria de Título. Departamento de Geología y Geofísica, Universidad de Chile (279 p.).

Benavente, O., 2015. Origen y naturaleza de los fluidos en los sistemas volcánicos e hidrotermales activos de los Andes de Chile Central (32.5–36°S). Doctoral Thesis. Departamento de Geología, Universidad de Chile (In Spanish).

Benavente, O., Tassi, F., Reich, M., Aguilera, F., Capecchiacci, F., Gutiérrez, F., Vaselli, O., Rizzo, A., 2015. Chemical and isotopic features of cold and thermal fluids discharged in the Southern Volcanic Zone between 32.5S and 36S: Insights into the physical and chemical processes controlling fluid geochemistry in geothermal systems of Central Chile. Chem. Geol. http://dx.doi.org/10.1016/j.chemgeo.2015.11.010.

Charrier, R., Wyss, A.R., Flynn, J.J., Swisher III, C.C., Norell, M.A., Zapatta, F., Mckenna, M.C., Novacek, M.J., 1996. New evidence for Late Mesozoic–Early Cenozoic evolution of the Central Chile. J. S. Am. Earth Sci. 9, 393–422. http://dx.doi.org/10.1016/S0895-9811(96)00035-1.

Charrier, R., Baeza, O., Elgueta, S., Flynn, J., Gans, P., Kay, S., Muñoz, N., Wyss, A., Zurita, E., 2002. Evidence for Cenozoic extensional basin development and tectonic inversion south of the flat-slab segment, southern Central Andes, Chile (33°–36°S.L.). J. South Am Earth Sci. 15, 117–139. http://dx.doi.org/10.1016/S0895-9811(02)00009-3.

Charrier, R., Bustamante, M., Comte, D., Elgueta, S., Flynn, J.J., Iturra, N., Muñoz, N., Pardo, M., Thiele, R., Wyss, A.R., 2005. The Abanico extensional basin: regional extension, chronology of tectonic inversion and relation to shallow seismic activity and Andean uplift. Neues Jahrb. Geol. Palaeontol. Abh. 236, 43–77.

Clavero, J., Pineda, C., Mayorga, C., Giavelli, A., Aguirre, I., Simmons, S., Martini, S., Soffia, J., Arriaza, R., Polando, E., Achurra, L., 2011. Geological, geochemical, geophysical and first drilling data from Tinguiririca geothermal area, Central Chile. Geothermal Resources Council Transactions (GRC) vol. 35. Geothermal Resources Council, San Diego, California, pp. 731–734.

Combs, J., Hadley, D., 1977. Microearthquake investingations of the Mesa geothermal anomaly, Imperial Valley, California. Geophysics vol. 42, 17–33.

De Matteis, R., Vanorio, T., Zollo, A., Ciuffi, S., Fiordelisi, A., Spinelli, E., 2008. Three-dimensional tomography and rock properties of the Larderello-Travale geothermal area Italy. Phys. Earth Planet. Inter. 168, 37–48. http://dx.doi.org/10.1016/j.pepi.2008.04.019.

Farías, M., Comte, D., Charrier, R., Martinod, J., David, C., Tassara, A., Tapia, F., Fock, A., 2010. Crustal-scale structural architecture in central Chile based on seismicity and surface geology: Implications for Andean mountain building. Tectonics 29.

Foulger, G., 1982. Geothermal exploration and reservoir monitoring using earthquakes and the passive seismic method. Geothermics 11 (4), 259–268. http://dx.doi.org/10.1016/0375-6505(82)90032-3.

Foulger, G.R., Miller, A.D., 1995. Three-dimensional Vp and Vp/vs structure of the Hengill Triple Junction and geothermal area, Iceland, and the repeatability of tornographic inversion. Geophys. Res. Lett. 22 (10), 1309–1312. http://dx.doi.org/10.1029/94GL03387.

Foulger, G.R., Julian, B.R., Pitt, A.M., Hill, D.P., Malin, P.E., Shalev, E., 2003. Three-dimensional Crustal Structure of Long Valley Caldera, California, and Evidence for the Migration of CO_2 under Mammoth Mountain. 108 pp. 1–16. http://dx.doi.org/10.1029/2000JB000041.

Giggenbach, W.F., 1987. Redox processes governing the chemistry of fumarolic gas discharges from White Island New Zealand. Appl. Geochem. 2, 143–161. http://dx.doi.org/10.1016/0883-2927(87)90030-8.

Goff, F., Janik, C.J., 2000. Geothermal Systems. Encyclopedia of Volcanoes. In: Sigurdsson, H., Houghton, B., McNutt, S., Rymer, H., Stix, J. (Eds.), Academic Press, San Diego, CA, pp. 817–834.

Gonzales-Ferrán, O., 1995. Volcanes de Chile. Instituto Geográfico Militar, Santiago (639 pp.).

Hauser, A., 1997. Catastro y caracterización de las fuentes de aguas minerales y termales de Chile Santiago, Chile, Servicio Nacional de Geología y Minería (SERNAGEOMIN) (In Spanish) Boletín 50 (70 p.).

Husen, S., Smith, R.B., Waite, G.P., 2004. Evidence for gas and magmatic sources beneath the Yellowstone volcanic field from seismic tomographic imaging. J. Volcanol. Geotherm. Res. 131 (3-4), 397–410. http://dx.doi.org/10.1016/S0377-0273(03)00416-5.

Jousset, P., Haberland, C., Bauer, K., Arnason, K., 2011. Hengill geothermal volcanic complex (Iceland) characterized by integrated geophysical observations. Geothermics 40 (1), 1–24. http://dx.doi.org/10.1016/j.geothermics.2010.12.008.

Klein, F.W., 1978. Hypocenter location program HYPOINVERSE. U.S. Geol. Surv. Open File Rep. 78–694.

Kley, J., Monaldi, C.R., Salfity, J.A., 1999. Along-strike segmentation of the Andean foreland: causes and consequences. Tectonophysics 301, 75–94. http://dx.doi.org/10.1016/S0040-1951(98)90223-2.

Koulakov, I., 2013. Studying deep sources of volcanism using multiscale seismic tomography. J. Volcanol. Geotherm. Res. 257, 205–226. http://dx.doi.org/10.1016/j.jvolgeores.2013.03.012.

Lees, J.M., 2007. Seismic tomography of magmatic systems. J. Volcanol. Geotherm. Res. 167, 37–56. http://dx.doi.org/10.1016/j.jvolgeores.2007.06.008.

Lira, E., 2010. Estudio de Sismicidad, Tomografía Sísmica y Modelo de Física de Rocas: Potencial Sistema Geotermal asociado al Complejo Volcánico Tinguiririca, Master Thesis. Energía Andina Universidad de Chile.

Mescua, J.F., Giambiagi, L.B., Tassara, A., Gimenez, M., Ramos, V.A., 2014. Influence of pre-Andean history over Cenozoic foreland deformation: structural styles in the Malargue fold-and-thrust belt at 35°S, Andes of Argentina. Geosphere 10 (3), 585–609. http://dx.doi.org/10.1130/GES00939.1.

Mosolf, J.G., 2013. Stratigraphy, structure and geochronology of the Abanico Formation in the Principal Cordillera. Central Chile: evidence of protracted volcanism and implications for Andean Tectonics. PhD Thesis, University of California.

Muksin, U., Bauer, K., Haberland, C., 2013. Seismic Vp and Vp/Vs structure of the geothermal area around Tarutung (North Sumatra, Indonesia) derived from local earthquake tomography. J. Volcanol. Geotherm. Res. 260, 27–42. http://dx.doi.org/10.1016/j.jvolgeores.2013.04.012.

Muksin, U., Haberland, C., Nukman, M., Bauer, K., Weber, M., 2014. Journal of Asian Earth Sciences detailed fault structure of the Tarutung Pull-Apart Basin in Sumatra, Indonesia, derived from local earthquake data. J. Asian Earth Sci. 96, 123–131. http://dx.doi.org/10.1016/j.jseaes.2014.09.009.

Nukman, M., Moeck, I., 2013. Journal of Asian Earth Sciences structural controls on a geothermal system in the Tarutung Basin, North Central Sumatra. J. Asian Earth Sci. 74, 86–96. http://dx.doi.org/10.1016/j.jseaes.2013.06.012.

Ramos, V.A., Zapata, T., Cristallini, E.O., Introcaso, A., 2004. The Andean thrust system—latitudinal variations in structural styles and orogenic shortening. In: McClay, K. (Ed.), Thrust Tectonics and Hydrocarbon System. AAPG Mem., pp. 30–50.

Roecker, S.W., 1982. Velocity structure of the Pamir-Hindu Kush region: possible evidence of subducted crust. J. Geophys. Res. 87, 945–959. http://dx.doi.org/10.1029/JB087iB02p00945.

Roecker, S.W., Yen, Y.H., Tsai, Y., 1987. Three dimensional P and S wave velocity structure beneath Taiwan: deep structure beneath an arc- continent collision. J. Geophys. Res. 92, 547–570. http://dx.doi.org/10.1029/JB092iB10p10547.

Roecker, S.W., Sabitova, T.M., Vinnick, L.P., Burmakov, Y.A., Golvanov, M.I., Mamatkanova, R., Murinova, L., 1997. Three dimensional elastic wave velocity structure of the western and central Tien Shan. J. Geophys. Res. 98, 779–796. http://dx.doi.org/10.1029/93JB01560.

Rossel, P., Oliveros, V., Mescua, J., Tapia, F., Ducea, M.N., Calderón, S., Charrier, R., Hoffman, D., 2014. The Upper Jurassic volcanism of the Río Damas-Tordillo Formation (33°–35.5°S): insights on petrogenesis, chronology, provenance and tectonic implications. Andean Geol. 41 (3), 529–557. http://dx.doi.org/10.5027/andgeoV41n3-a03.

Simiyu, S.M., 1999. Seismic velocity analysis in the Olkaria geothermal field. 24th Workshop on Geothermal Reservoir Engineering. Standford University, Stanford, California, pp. 25–27 (January).

Spica, Z., Legrand, D., Iglesias, A., Walter, T.R., Heimann, S., Dahm, T., Pardo, M., 2015. Hydrothermal and magmatic reservoirs at Lazufre volcanic area, revealed by a high-resolution seismic noise tomography. Earth Planet. Sci. Lett. 421, 27–38. http://dx.doi.org/10.1016/j.epsl.2015.03.042.

Stern, C., Moreno, H., López-Escobar, L., Clavero, J., Lara, L.E., Naranjo, J.A., Parada, M.A., Skewes, M.A., 2007. Chilean volcanoes. In: Moreno, T., Gibbons, W. (Eds.), The Geology of Chile. Geological Society, London, pp. 147–178.

Tapia, F., 2015. Evolución tectónica de los Andes Centrales del sur durante el Cenozoico Superior (34°45′–35°30′S). Departamento de Geología, Universidad de Chile, Doctoral Thesis (In Spanish).

Thierer, P.O., Flueh, E.R., Kopp, H., Tilmann, F., Comte, D., Contreras, S., 2005. Local earthquake monitoring offshore Valparaiso Chile. N. Jb. Geol. Paläont. (Abh.) 236, 173–183.

Ward, P.L., Jacob, K.H., 1971. Micro earthquake in the Ahuachapan geothermal field. El Salvador, Central America. Science vol. 173, 328–330. http://dx.doi.org/10.1126/science.173.3994.328.

Yoshikawa, M., Sudo, Y., 2004. Three dimensional seismic velocity structure beneath the Otake-Hatchobaru geothermal area at Kuju volcano in central Kyushu, Japan. Ann. Disaster Prev. Res. Inst., Kyoto Univ. 47B.

Zhao, D., 2001. New advances of seismic tomography and its applications to subduction zones and earthquake fault zones. Island Arc 10, 68–84. http://dx.doi.org/10.1046/j.1440-1738.2001.00291.x.